Macromolecules

pubs.acs.org/Macromolecules Article

Structure of the Poly(methyl methacrylate) Adsorbed Layer Determined by the Surface Chemistry of the Substrate

Weizhao Ren, Yongming Hong, Huidong Wei, Jianquan Xu,* Cuiyun Zhang, Xianjing Zhou, and Xinping Wang*

Cite This: https://doi.org/10.1021/acs.macromol.2c02169 Read Online

ACCESS | Metrics & More | Article Recommendations | Supporting Information

ABSTRACT: The adsorbed polymer layer on the inorganic solid surface is crucial in improving the physical properties of composite nanomaterials; therefore, the properties could be tuned by altering the structure of the adsorbed layer. We investigated poly(methyl methacrylate) (PMMA) adsorbed layers on SiO_2−Si substrates by varying the hydroxyl (OH) group content on the substrate surface. The results indicated that the thicknesses of the flattened layer and loosely adsorbed layer decreased with decreasing OH group content and the flattened layer disappeared when the content was ∼31%. The OH groups controlled the formation of the adsorbed layer, providing anchor points through hydrogen bonding with the carbonyl groups in PMMA. With decreasing OH group content, fewer anchor points possibly prevented train conformation and the relatively stable loosely adsorbed chains still formed, which enhanced the segmental dynamics of the ultrathin PMMA film. These results provide novel insight into the role of surface chemistry in forming adsorbed polymer layers on substrates.

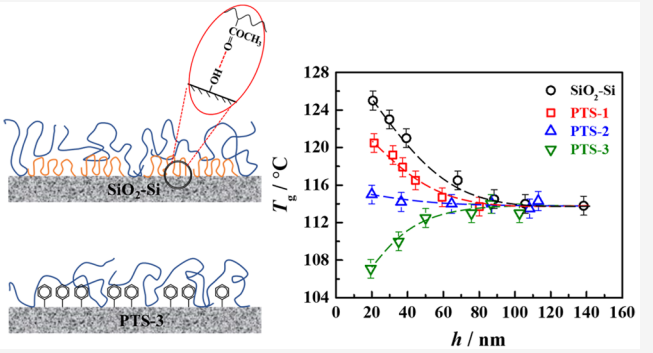

INTRODUCTION

The polymer/solid interface plays a crucial role in a wide field of nanoscience and nanotechnology involving physics, chemistry, biology, and engineering. Recently, an increasing number of experimental results have revealed that the physical properties of nanoconfined polymer materials are controlled by the irreversibly adsorbed polymer layers on solid surfaces.[1−11] For example, the size of loops in adsorbed chains on a solid surface has been found to be responsible for controlling the dynamics of a supported polymer thin film.[4,5] Furthermore, the propagation distance associated with the substrate effect has been found to increase in direct proportion to the thickness of the adsorbed layer.[6,7] Therefore, by adjusting the structure of the adsorbed layers, tailoring the physical properties of nanomaterials, such as glass transition temperature, thermal expansion coefficient, viscosity, crystallization, and wettability, is possible. Because of its significance, the structure of the adsorbed polymer layer on the solid substrate has been widely investigated by Koga and co-workers.[2,12−14] They revealed that the adsorbed layer contains two regions: the inner high-density region with more flattened chain conformation (flattened layer) and the outer bulk-like density region with bulk-like chain conformation (loosely adsorbed layer). The flattened layer forms as a result of the high number of contacts between the inner chains and the substrate, whereas the loosely adsorbed layer is formed by the loosely adsorbed chains that form larger loops.[14] Additionally, the thickness of the flattened layer is independent of molecular weight, whereas the thickness of the outer loosely adsorbed layer increases with molecular weight.[12]

To adjust the structure of adsorbed layers, understanding the process of irreversible adsorption of polymer chains on the solid surface is crucial. Napolitano and co-workers have made major contributions to the study of irreversible chain adsorption kinetics.[15−17] Two adsorption processes have been observed: linear growth of the adsorbed layer thickness over short periods and logarithmic growth over long periods.[15] In previous studies,[12,18,19] a flattened layer of polystyrene (PS) on a substrate exhibited power-law evolution during the early stage of the adsorption process and reached a quasi-equilibrium platform of 2.1 nm in thickness when the annealing time (t_{an}) was >4 h at 150 °C. Meanwhile, the thickness of the entire adsorbed layer (including the flattened layer and loosely adsorbed layer) showed similar power-law growth within approximately 4 h and then shifted to a sluggish logarithmic growth until a maximum value was achieved at t_{an} > 96 h. Because the crossover time (t_c ∼ 4 h) for the adsorbed

Received: October 22, 2022
Revised: January 15, 2023

layer was similar to that of the flattened layer, these two diverse chain conformations (flattened chains and loosely adsorbed chains) were considered to occur and grow independently on the substrate surface. The formation of the flattened layer prior to t_c is attributed to a "collapse and zipping-down" process on the substrate surface.[20,21] Further rearrangement of the flattened chains toward a quasi-equilibrium state was caused by an increase in the number of contacts between the substrate surface and segments, which overcame the conformation entropy loss.[12,14,22] This caused the flattened layer thickness to increase with annealing time during the early stage.

Although polymer chains that form the loosely absorbed layer can also be adsorbed at $t < t_c$, their arrival is delayed owing to a diffusion-controlled mechanism; thus, their adsorption is suppressed because the flattened chains have already occupied the majority of the substrate surface. Hence, the loosely adsorbed polymer chains have to form bridge connections among the nearly empty sites.[20] The flattened chains and late-arriving chains continue to compete for adsorption until the substrate surface is fully covered at $t = t_c$. When $t > t_c$, along with the termination of the formation of the flattened layer, the late-arriving chains produce the loosely adsorbed layer via a "reeling-in" process that dominates the chain adsorption behavior. This process is considerably slow because of the excluded-volume repulsion from previously adsorbed chains and because the chains may entangle with adjacent free chains. Consequently, a logarithmic increase in the thickness of the adsorbed layer occurs before reaching the final state.

A previous study has shown that the polymer−substrate interaction plays an important role in the formation of the adsorbed layer.[12] Moreover, the flattened layer thicknesses of three different polymers (PS, PMMA, and poly(2-vinylpyridine) (P2VP)) on SiO_2−Si substrates increased with increasing polymer−substrate interactions, whereas the adsorption kinetics showed an opposite trend. The flattened layer thickness and its surface coverage for PS were 2.1 nm and 75%, respectively, whereas those of P2VP were 3 nm and 90%, respectively. However, the effect of the substrate surface chemistry on the adsorbed layer structure remained ambiguous. A considerable amount of evidence indicates that the carbonyl (C═O) groups in polymers can form hydrogen bonds with the OH groups on a SiO_2−Si substrate surface.[23−25] Therefore, the OH groups on the substrate surface should be considerably important contact sites for forming the PMMA adsorbed layer on the SiO_2−Si substrate. Herein, to clarify the role of the OH groups on the substrate, the structures of PMMA layers adsorbed on SiO_2−Si substrates with various OH group contents were investigated by replacing OH groups with phenyl groups. The results indicate the significance of the OH group content in the final adsorbed layer structure at the solid−polymer interface.

EXPERIMENTAL SECTION

Materials. Monodisperse PMMA with two different molecular weights (PMMA-1: M_w = 278 kg mol^{-1}, polydispersity index (PDI) = 1.15; PMMA-2: M_w = 15 kg mol^{-1}, PDI = 1.10) were obtained from Polymer Source Inc. (Canada). Phenyltrimethoxysilane ($C_6H_5Si(OCH_3)_3$, PTS) was provided by Aldrich Co. (USA). Silicon (100) wafers with an approximately 2 nm native oxide layer (i.e., SiO_2−Si substrate), quartz windows, and half-cylinder quartz prism were employed as substrates for ellipsometry and sum frequency generation (SFG) vibrational spectroscopy measurements. Before preparing the polymer films, all substrates were washed with a piranha solution (H_2SO_4:H_2O_2 = 3:1 [v/v]), as reported previously.[26]

Preparation of the Adsorbed Layer on Substrates with Various OH Group Contents. The substrates with various OH group contents were prepared by replacing OH groups with phenyl groups based on previous reports.[26,27] After exposing the cleaned SiO_2−Si substrates to the PTS solution for different times, PTS was bonded to the surface via the reaction between the OH and −Si−OCH_3 groups. Consequently, the substrate surfaces presented different OH group contents. The OH group-controlled substrates were further analyzed via water contact angle (WCA) measurements, X-ray photoelectron spectroscopy (XPS), and SFG according to the procedures in our recent reports.[26,27] Using the Cassie equation,[26,28] the fraction of OH groups on the substrate surface can be roughly calculated based on the WCA results. Substrates with OH group coverages of 80, 51, and 31% were used and labeled PTS-1, PTS-2, and PTS-3, respectively.

PMMA thin films (thickness > 8 R_g, where R_g is the gyration radius of the polymer chain) were produced by spin-coating a 4 wt % toluene solution of PMMA onto the substrates. Subsequently, the PMMA films were annealed at T_g + 75 °C (T_g is the glass transition temperature of the polymer) for 72 h to form the adsorbed layer in the final state. Thereafter, the annealed films were leached several times using DMF or toluene according to the reported procedure.[29] The thicknesses of the PMMA films and adsorbed layers were determined by ellipsometry (Accurion GmbH, Germany).

Characterization. The surface topography of the adsorbed layer was presented via atomic force microscopy (AFM, MultiMode-8, Bruker, USA) in air using the tapping mode and a tip with a spring constant of 40 N m^{-1}. X-ray reflectivity (XRR) was chosen to determine the density distribution in the adsorbed layers, as previously reported.[8,12] XRR was conducted at the BL14B1 beamline (the wavelength of X-rays, λ, is 1.2398 Å) of the Shanghai Synchrotron Radiation Facility (SSRF, China). The evolution of X-ray reflectivity with its incident angle (θ) was detected, and the curve of specular reflectivity was plotted as a function of the scattering vector (q_z) in a direction perpendicular to the surface ($q_z = 4\pi(\sin\theta)/\lambda$). A multilayer model was employed to fit this plot to obtain the mass density profile. The thicknesses and T_g values of the thin PMMA films and the adsorbed layers (i.e., the flattened layer and interfacial sublayer) supported on different substrates were determined by EP^{4}SW imaging ellipsometry (Accurion GmbH Co., Germany) with a variable wavelength laser source and 658 nm laser source. The value of T_g could be obtained from the turning temperature by changing the thermal expansion coefficients from the glassy to rubbery state. The detail of ellipsometry measurement is shown in the Supporting Information. Figure S1 shows that no glass transition could be observed within the temperature range from 40 to 160 °C for the interfacial sublayer and flattened layer, which indicates much slower chain mobility of adsorbed chains than that in the bulk (T_g^{bulk} is 114 °C for PMMA-1).

To collect vibrational signals originating from the adsorbed layer at the PMMA/substrate interface, a sandwiched geometry was employed for SFG measurements (EKSPLA Co., Lithuania), as reported previously.[4,27,30,31] Both the fused quartz window and half-cylinder prism with various OH contents were deposited on a spin-coated PMMA-1 film (~200 nm). The quartz window and half-cylinder prism were stacked and annealed at 120 °C under vacuum using a vacuum oven with a mechanical pump for 12 h to remove the excess solvent. The samples were then annealed at 190 °C for 72 h under the experimental conditions. Incident angles of 53° and 60° were used for the tunable infrared (IR) beam and the visible (Vis) beam at 532 nm, respectively. The beams of 50 Hz and ~30 ps pulse width were pumped by the fundamental outputs of the laser and the secondary harmonic. The SFG spectra for the s-polarized SFG signal, s-polarized Vis and p-polarized IR (*ssp*), and the p-polarized SFG signal, p-polarized Vis and p-polarized IR (*ppp*), were collected. The SFG spectra were recompensated by the Vis and IR input energy, and then the SFG signal was fitted using the following Lorentzian equation:

https://doi.org/10.1021/acs.macromol.2c02169
Macromolecules XXXX, XXX, XXX−XXX

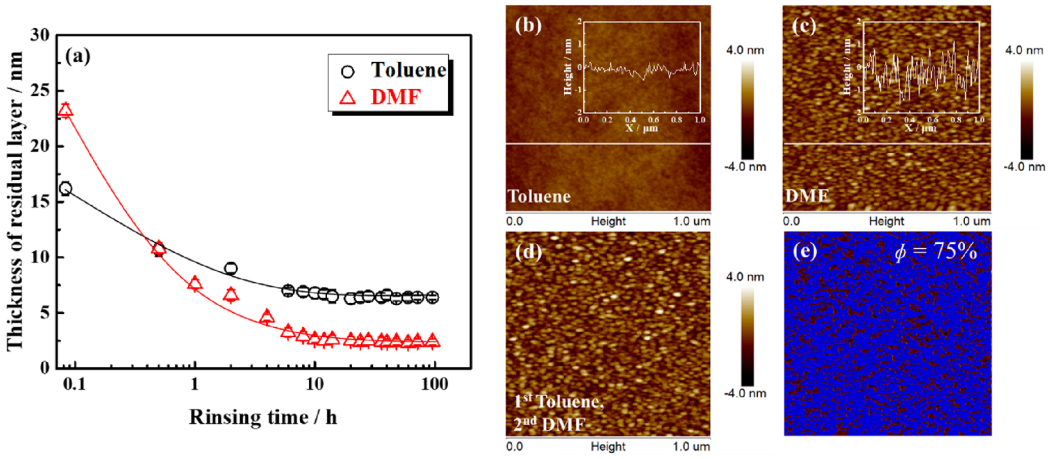

Figure 1. (a) Change in residual thickness of PMMA-1 on the SiO_2−Si substrate with rinsing time using toluene and DMF as leaching solvents. AFM height images (scan size: 1 μm × 1 μm; height scale: −4 to 4 nm) of the PMMA adsorbed layer on the SiO_2−Si substrate obtained via rinsing with (b) toluene, (c) DMF, and (d) the sample shown in panel (b) subsequently leached using DMF. (e) Corresponding bearing area analysis result for the AFM image shown in panel (c). The blue area shows the space occupied by the polymer chains. The corresponding height profiles along the white line in panels (b) and (c) are plotted in the insets.

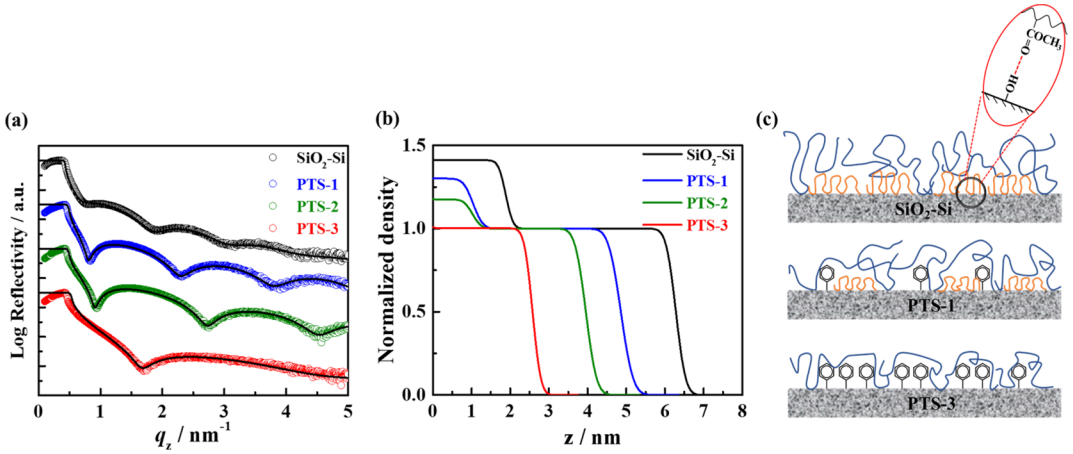

Figure 2. (a) X-ray reflectivity (XRR) profiles as a function of scattering vector (q_z) for the PMMA-1 interfacial sublayer on substrates with various OH group contents obtained via toluene leaching (open symbols: experimental data; solid lines: best fits). (b) Normalized density profiles for the PMMA-1 interfacial sublayer on SiO_2−Si substrates with various OH group contents plotted as a function of the distance (z) from the substrate surface. (c) Schematic illustrations to show the chain conformations on different substrate surfaces (blue: loosely adsorbed chains; orange: flattened chains).

$$I_{SFG} \propto |\chi^{(2)}_{eff}|^2 = \left|\chi^{(2)}_{NR} + N\sum_q \frac{A_q}{\omega_{IR} - \omega_q + i\Gamma_q}\right| \quad (1)$$

where I_{SFG} and $\chi^{(2)}_{eff}$ are the intensity of the SFG signal and the effective second-order nonlinear susceptibility, respectively, and $\chi^{(2)}_{NR}$, N, ω_q, A_q, and Γ_q are the nonresonant contribution, molecular density on the interface, resonance frequency, strength, and damping coefficients of the q resonant vibrational mode, respectively. A_q and Γ_q were obtained by fitting the SFG signal with the Lorentzian equation.

RESULTS AND DISCUSSION

Structure of the PMMA Adsorbed Layer on the SiO_2−Si Substrate. The final adsorbed layers are typically described as being in a quasi-equilibrium state[12,15−17,32] in which the thickness remains unchanged with the change in annealing time. As reported in previous studies, the entire adsorbed layer can be assigned as the interfacial sublayer,[12,33] which consists of the inner flattened chains and outer loosely adsorbed chains. To obtain the PMMA interfacial sublayer on the SiO_2−Si substrate, the spin-cast PMMA-1 films (~200 nm) were annealed at 190 °C (~T_g + 75 °C) for up to 72 h. The thickness of the adsorbed layer remained unchanged when the annealing time was >30 h (see Figure S2). In this study, the adsorbed layer was obtained after annealing for 72 h to achieve a quasi-equilibrium state, which was considerably >30 h. Toluene and DMF were employed during the leaching process to obtain the interfacial sublayer and flattened layer, respectively. Figure 1a shows the change in the residual layer thickness with increasing leaching time using toluene and DMF. The thicknesses of the adsorbed layers on SiO_2−Si were 6.3 ± 0.4 nm for toluene leaching and 2.4 ± 0.2 nm for DMF leaching at equilibrium, which correspond to the thicknesses of the interfacial sublayer[34] and flattened layer[12] of PMMA on the SiO_2−Si substrate, respectively. These thicknesses were further confirmed via AFM (see Figure S3).

The AFM height image (Figure 1b) indicated that the adsorbed layer obtained after toluene leaching was smooth.

https://doi.org/10.1021/acs.macromol.2c02169
Macromolecules XXXX, XXX, XXX−XXX

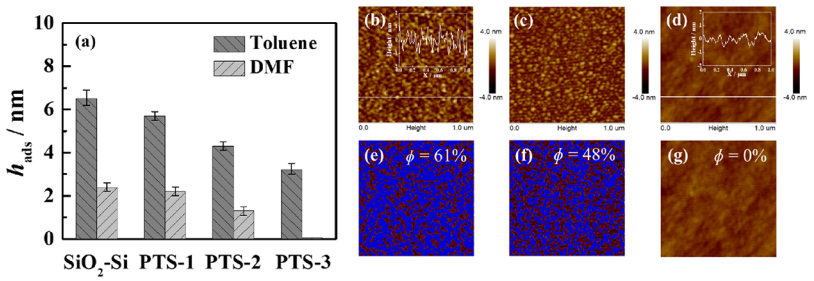

Figure 3. (a) Thicknesses (h_{ads}) of the PMMA-1 adsorbed layer on substrates with various OH group contents obtained via toluene and DMF leaching. AFM height images (scan size: 1 μm × 1 μm; height scale: −4 to 4 nm) of the PMMA-1 flattened layer on (b) PTS-1, (c) PTS-2, and (d) PTS-3 substrates. Bearing area analysis results for the AFM images in panels (b), (c), and (d) are shown in panels (e), (f), and (g), respectively. The blue area shows the space occupied by the polymer chains. The corresponding height profiles along the white line in panels (b) and (d) are plotted in the insets.

However, the adsorbed layer obtained after DMF leaching showed an "island" shape (Figure 1c). When the sample shown in Figure 1b was further leached using DMF, the thickness of the adsorbed layer decreased to 2.4 ± 0.2 nm and the morphology also showed an "island" shape (Figure 1d). These results are consistent with those of the PS adsorbed layer on the SiO_2−Si substrate previously reported.[12,35−37] These results indicate that the PMMA adsorbed layer on SiO_2−Si obtained via toluene leaching consisted of a two-layer structure: a flattened layer and loosely adsorbed layer, namely, the interfacial sublayer. Conversely, the PMMA adsorbed layer on SiO_2−Si obtained via DMF leaching consisted only of the flattened layer. The Hansen solubility parameters of toluene and DMF[38] are as follows: δ_d = 18.0, δ_p = 1.4, and δ_h = 2.0 for toluene and δ_d = 17.4, δ_p = 13.7, and δ_h = 11.3 for DMF, where δ_d, δ_p, and δ_h are the contributions of dispersive, polar, and hydrogen bonding, respectively. Because DMF has stronger interactions with the SiO_2−Si substrate than toluene, it could readily remove the outer loosely adsorbed chains in the interfacial sublayer, allowing the lone flattened layer to emerge more effectively. AFM height images and nanoscope analysis software (Bruker) were used to estimate the surface coverage (ϕ) (i.e., the area percentage occupied by the polymer chains) of the PMMA flattened layer on the substrates above a critical threshold (0 nm in the AFM height images). Figure 1e shows the representative surface coverage analysis results of the AFM images from Figure 1c. The estimated ϕ was 75 ± 4%, which is in good agreement with that reported by Koga et al.[12] This result indicates that the interfacial sublayer and flattened layer of PMMA in a quasi-equilibrium state can be successfully obtained via leaching using toluene and DMF.

Figure 2 displays the XRR curves and normalized density profiles of the PMMA-1 interfacial sublayer in a quasi-equilibrium state on various substrates. For the fitting of XRR data, a four-layer model of Si/SiO_2/high-density PMMA/bulk-like density PMMA and a three-layer model of Si/SiO_2/adsorbed PMMA layer were both employed by using Igor Pro, and the fitting results are shown in Tables S1 and S2. The detail for the fitting is displayed in the Supporting Information. It is found that a four-layer model was preferable for SiO_2-Si, PTS-1, and PTS-2 substrates, while a three-layer model was preferable for the PTS-3 substrate. The best fits are plotted in Figure 2a. Hence, the density distribution profiles (Figure 2b) indicate that the adsorbed layer consisted of a high-density region near the substrate and a bulk-like density region on the exterior. The value of the flattened layer thickness obtained via DMF leaching (Figure S4) was almost the same as the thickness of the high-density layer within the experimental error. Additionally, its density was homogeneous. Therefore, these results further demonstrate that the flattened layer was successfully extracted via DMF leaching. With the increase in substrate surface phenyl fraction from 0 to 69% (substrate changes from SiO_2-Si to PTS-3), the thicknesses of the flattened layer and interfacial sublayer both decreased, and even no flattened layer could be observed on the PTS-3 substrate. Figure 2c shows the schematic illustrations of the thicknesses and conformations of adsorbed chains on different phenyl fraction substrates.

Effect of Substrate Surface OH Group Content on the Structure of the Adsorbed PMMA Layer. Generally, PMMA has strong interactions with SiO_2−Si surfaces because of hydrogen bond interactions between the C═O groups in PMMA chains and OH groups on SiO_2−Si surfaces. To investigate the effect of the substrate OH group content on the structure of the adsorbed PMMA layer, substrates were prepared and characterized with surface phenyl group contents of 0% (i.e., SiO_2−Si substrate), 20% (PTS-1), 49% (PTS-2), and 69% (PTS-3), as previously described.[26] Because the OH groups were substituted by phenyl groups, the corresponding OH group contents on the SiO_2−Si surfaces were 100, 80, 51, and 31%, respectively. The phenyl groups on the SiO_2−Si surface were homogeneous, as previously demonstrated by C1s XPS and SFG studies.[26]

Figure 3a further shows the thicknesses of the PMMA-1 interfacial sublayer and flattened layer on substrates with various OH group contents. With decreasing surface OH group content from 100 to 31%, the interfacial sublayer thickness decreased from 6.3 ± 0.4 to 3.2 ± 0.3 nm, respectively, and the flattened layer thickness decreased from 2.4 ± 0.2 to 0 nm, respectively. Furthermore, the surface coverage of the flattened layer decreased from 75 to 0% at the same time (Figure 3b−g). It is believed that the increased content of the phenyl groups on the substrate prevents the flattening process, making it more difficult to form a flattened layer, resulting in a thinner flattened layer and lower coverage of the flattened layer.

The density distributions of the PMMA-1 adsorbed layer on substrates with various OH group contents along the normal direction of the substrate surface are shown in Figure 2b. The PMMA chains near the SiO_2−Si substrate surface may have adopted a compact conformation to form the flattened adsorbed layer,[14,18,35] resulting in a denser layer than the bulk. It has been reported that the density of the adsorbed layer was about 20−50% higher than the bulk by using X-ray

https://doi.org/10.1021/acs.macromol.2c02169
Macromolecules XXXX, XXX, XXX−XXX

reflectivity, neutron reflectivity, and computer simulations,[14,39,40] which were consistent with our results. However, the thickness and density of the flattened layer decreased with decreasing OH group content. When the OH group content on the SiO_2−Si surface was 31% (PTS-3), the relatively high-density layer (i.e., flattened layer) disappeared and the interfacial sublayer was a single-layer structure. This was in good agreement with the results shown in Figure 3.

Figure 4 shows the effect of substrate surface chemistry on the T_g of the supported PMMA-1 thin films. Similar to the

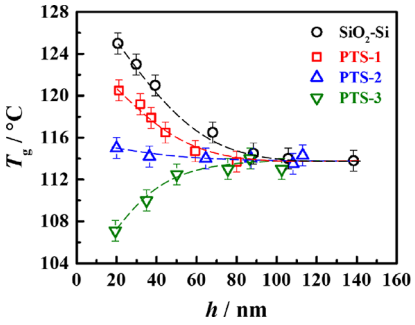

Figure 4. Glass transition temperature (T_g) of thin PMMA-1 films supported on substrates with various OH contents as a function of film thickness (h).

reported results,[41,42] the T_g of the thin PMMA film supported by the SiO_2−Si substrate increased with decreasing film thickness. However, the enhancement of T_g of the ultrathin PMMA film decreased with decreasing OH content on the substrate surface. When the OH content was 31% (PTS-3), the T_g of the supported PMMA thin film decreased with decreasing film thickness. Similar to our previous reports,[4−7] this result further demonstrates that the dynamics of the supported polymer thin film could be adjusted by changing the surface chemistry of the substrate, which changes the structure of the adsorbed layer. The previously observed[26,27] anchoring effect of the polymer chains pinned to the substrate surface via $\pi-\pi$ interactions could suppress segmental mobility and afford an increase in T_g values for the PS thin films. Therefore, we hypothesized that the OH group content on the substrate surface could affect the anchoring of PMMA chains, thus changing the structure of the adsorbed layer.

To investigate the chain structure of the adsorbed layer on the substrates with various OH group contents, a sandwiched geometry was employed for the SFG measurements to measure the SFG signal at the PMMA/SiO_2 interfaces and further study the chain conformation. The details of the sandwiched geometry were reported previously.[4,26,31] Figure 5 shows the *ssp* and *ppp* SFG spectra within the wavenumber range from 2850 to 3100 cm^{-1} for the PMMA adsorbed layer on substrates with various OH group contents. In the *ssp* SFG spectra (Figure 5a), the intensities of the peaks at 2910 and 3060 cm^{-1} increased and the intensity of the peak at 2955 cm^{-1} decreased with decreasing OH content on the substrate surface. However, in the *ppp* SFG spectra of the PMMA adsorbed layer (Figure 5b), only a peak at 2957 cm^{-1} was found for the SiO_2−Si substrate. When the substrate was modified by the phenyl groups, peaks at 2990, 3020, and 3060 cm^{-1} were observed, the intensities of which increased with decreasing OH group content (from 80 to 31%) on the substrate.

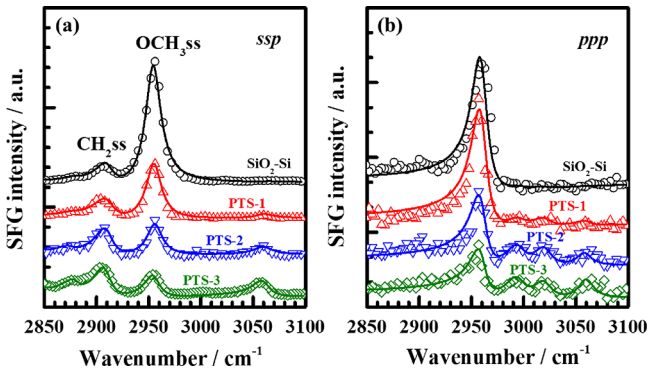

Figure 5. The *ssp* (a) and *ppp* (b) SFG spectra collected from the PMMA-1 adsorbed layer on substrates with various OH contents. The solid lines are the best-fitted curves, and the fitting parameters are listed in Table S3. The spectra are offset for clarity.

According to the references for peak assignments of the *ssp* SFG PMMA spectra,[25,43−47] the peaks at 2910 and 2955 cm^{-1} are attributed to the C−H symmetric stretching vibrations of the methylene groups (CH_2) and ester methyl groups (OCH_3), respectively. The peak at ∼3060 cm^{-1} is attributed to the ν_2 stretching mode of aromatic groups,[48−50] which results from phenyl groups on the SiO_2 surface, as confirmed by our previous report.[26] In the *ppp* SFG spectra, the peaks at approximately 2957 and 3020 cm^{-1} originate from the C−H symmetric and asymmetric stretching vibrations of the OCH_3 groups within the experimental error. The C−H asymmetric stretching vibrations from both the α methyl and OCH_3 groups produce signals at 2990 cm^{-1}. The SFG spectra of the PMMA adsorbed layer on the SiO_2−Si substrate were similar to those reported by Tanaka et al.[25] for cast PMMA film surfaces on which hydrophobic methylene groups were present. The OCH_3 and CH_2 groups were perpendicular to the surface, whereas the α methyl group was parallel to the surface. Interestingly, the CH_2 C−H symmetric stretching peak at 2910 cm^{-1} increased with the suppression of the OCH_3 C−H symmetric stretching peak at 2955 cm^{-1} in the *ssp* SFG spectra, and both peaks at 2990 and 3020 cm^{-1} increased in the *ppp* SFG spectra for the phenyl-modified substrates, which were similar to the spin-coated film surface.[47] These results indicate that the OCH_3 groups were randomly oriented at the PMMA/phenyl-modified substrate interfaces.

To obtain the orientation of the OCH_3 groups, the average tilt angle of the OCH_3 groups relative to the normal of the substrate surface was estimated. Figure S5a shows the calculated curves of $|\chi_{eff,ssp,ss}^{(2)}/\chi_{eff,ppp,as}^{(2)}|$ with different tilt angles for the different distributions. Figure S5b shows the OCH_3 tilt angle as a function of the phenyl content. Three measurements were performed to obtain the error bar. The OCH_3 tilt angle was approximately 16° when the phenyl group content was 0%. The tilt angle increased with increasing phenyl group content. When the phenyl content increased to ∼69%, the tilt angle increased to ∼45°. These results indicate that the OCH_3 group presents an upright orientation relative to the substrate and exhibits a more reclining orientation with increasing phenyl group content. As reported previously,[51] the orientation of the OCH_3 group is related to the conformation of the adsorbed PMMA chain, which could be adjusted by the OH group content on the substrate surface.

https://doi.org/10.1021/acs.macromol.2c02169
Macromolecules XXXX, XXX, XXX−XXX

Lu and Li[52] reported that the increase in peak intensity at 3060 cm^{-1} for the PS/sapphire interface was attributed to the formation of more train sequences on the substrate (i.e., flattened layer), and the SFG signal from loops could be ignored because the SFG signal was not produced at locations with ensemble-averaged inversion symmetry. The flattened layer with a train conformation provides a more ordered orientation of the pendant phenyl rings. The decreased peak intensity at 2955 cm^{-1} suggests that the main chain component was more disordered.[53] According to previous reports,[22,54] the adsorbed chains consist of three conformations: train, loop, and tail. The SFG signal is mainly attributed to the train conformation because it is sensitive to the local order at the interface where the symmetry of the polymer is disrupted.[52,55] Therefore, the before mentioned results indicate that the SFG spectra at the PMMA/SiO_2 interface were mainly a result of the train conformation in the flattened layer.

Figure 6 shows the *ssp* SFG spectra of the PMMA-1 adsorbed layer on the SiO_2−Si and PTS-3 (31% OH content) substrates within 1600−1800 cm^{-1}. The SFG spectrum from the PTS-3 substrate showed an intense peak at 1738 cm^{-1}, which was attributed to C═O stretching in the carbonyl group; however, the center of this peak was shifted to 1726 cm^{-1} and the 1738 cm^{-1} peak was reduced, creating a shoulder. A similar phenomenon was reported for poly(vinyl acetate) (PVAc) films supported on the phenyl group-modified SiO_2−Si substrate,[23] for which the increase in the 1720 cm^{-1} peak with increasing OH content on the substrate surface was caused by increased hydrogen bonding between the C═O groups in the PVAc chains and the OH groups on the substrate surface. From this result, we can deduce that decreasing the OH group content on the substrate surface reduced the hydrogen bonding between the C═O groups in the PMMA chains and the OH groups on the substrate surface, which decreased the number of anchor points for PMMA adsorption. Therefore, when the OH group content was 100%, the numerous OH groups acted as anchoring sites that promoted the formation of the train conformation (Figure 2c). This train conformation results in a well-ordered, folded main chain with well vertically oriented OCH_3 groups. Hence, a thicker interfacial sublayer (indicating a greater amount of adsorbed chains) was formed on the SiO_2−Si surface consisting of a thicker flattened layer with higher coverage and more loosely adsorbed chains. When many of the OH groups on the SiO_2−Si surface were replaced by phenyl groups, the phenyl groups prevented hydrogen bonding between the C═O and OH groups, thus, the development of the train conformation. The decrease in OH group content and the increase in distance between the OH groups acting as anchor points resulted in the formation of a loop conformation with long chains covering the phenyl groups (Figure 2c). Therefore, the OCH_3 C−H symmetric stretching decreased and the peaks at 2990 and 3020 cm^{-1} appeared in the *ppp* SFG spectra with decreasing OH group content on the substrate surface.

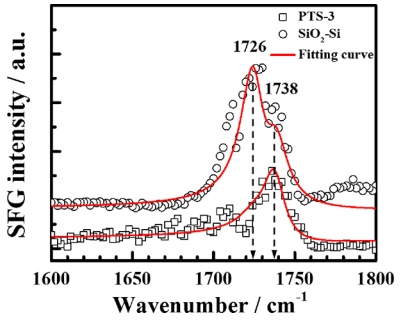

Figure 6. The *ssp* SFG spectra of the PMMA-1 adsorbed layer on the SiO_2−Si substrate (circle) and the substrate with 31% OH groups (PTS-3) (square).

The decrease in the flattened layer and interfacial sublayer thicknesses and the reduced coverage of the flattened layer with decreasing OH group content could be explained based on the mechanism of end-grafting chains.[56−58] "Stretched brushes" occur when the end-tethered polymer chains are grafted densely, and the brush height increases proportionally with the grafting density.[14,59,60] As previously reported,[29] the

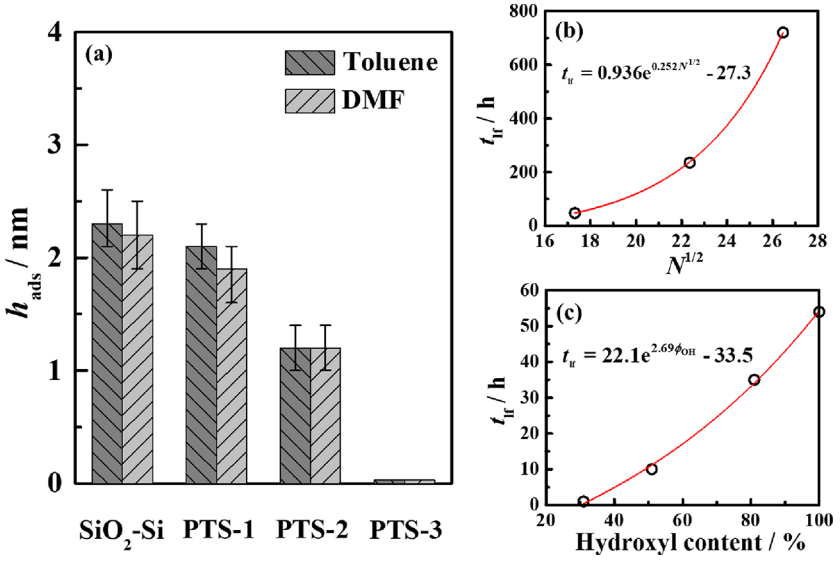

Figure 7. (a) Thicknesses (h_{ads}) of the PMMA-2 adsorbed layer on the substrates with various OH group contents obtained by toluene and DMF leaching. (b) Leaching time (t_{lf}) to obtain the flattened layer of PMMA on SiO_2−Si with molecular weights of 30, 50, and 70 kg/mol using toluene. (c) Leaching time to obtain the flattened layer of PMMA-1 on substrates with various OH group contents using DMF.

https://doi.org/10.1021/acs.macromol.2c02169
Macromolecules XXXX, XXX, XXX−XXX

irreversibly adsorbed polymer chains on the substrate could be regarded as "Guiselin" brushes, which have many contacts between the substrate and segments ($N^{1/2}$ contacts per chain, where N is the degree of polymerization). We postulated that the interfacial sublayer, which includes the inner flattened chains and outer loosely adsorbed chains, can be considered as dry brushes. Because the OH groups on the SiO_2−Si surface act as anchoring points for the adsorption of PMMA chains, the adsorbed PMMA chains easily formed the flattened layer with a train conformation and loosely adsorbed chains when the SiO_2−Si surface was covered by 100% OH groups (many anchoring points). This yielded a thicker interfacial sublayer and flattened layer and higher coverage of the flattened layer. In this case, when the content of the OH groups (i.e., anchoring points) on the substrate surface decreased, the adsorbed PMMA chain had difficulty in forming a flattened layer with a train conformation and leaving few anchoring sites for the late-arriving chains to form loosely adsorbed chains, resulting in a thinner interfacial sublayer and flattened layer and lower coverage of the flattened layer. That is, the reduced thicknesses of the interfacial sublayer and flattened layer with the lower OH group content were caused by a decrease in effective grafting density (i.e., the number of chain contacts with substrate per unit area). When the OH group content on the substrate surface was approximately 31%, the PMMA interfacial sublayer consisted of only loosely adsorbed chains, and the flattened layer with a train conformation cannot form.

Effect of Contact Sites on the Formation of the Loosely Adsorbed Chains. To confirm that the formation of the PMMA adsorbed layer was related to the anchoring point OH groups, PMMA-2 with a low molecular weight (15 kg/mol) was used. The number of anchoring points for one chain decreases with decreasing polymer molecular weight (schematic in Figure 2c), which facilitates the loosely adsorbed chains to be easily removed by the solvent. Figure 7a shows that the thicknesses of the adsorbed layers obtained using toluene and DMF were similar when the molecular weight of PMMA was 15 kg/mol. Figure S6 shows the AFM height images and surface coverages of the PMMA-2 flattened chains on various substrates. It is found that the morphology of PMMA-2 flattened chains is smooth and their surface coverages are almost 100%, which is different from those for PMMA-1 (see Figure 3) and consistent with the prediction of O'Shaughnessy and Vavylonis.[20] Because the chain/solid contacts for the irreversibly adsorbed polymer chains on the solid were considered $N^{1/2}$ contacts per chain,[17,29] the number of contacts for both the flattened chains and loosely adsorbed chains decreased with PMMA molecular weights. For PMMA with relatively low molecular weights, the loosely adsorbed chains were easily removed by the solvent owing to few anchoring points; therefore, similar adsorbed layers were obtained using toluene and DMF as leaching solvents (Figure 7a). This is likely why the molecular weight affects the thicknesses of the adsorbed layers obtained using both toluene and DMF. The thicknesses of the residual layers of the PMMA film on SiO_2−Si with molecular weights of 30, 50, and 70 kg/mol are presented in Figure S7a as a function of toluene leaching time. The leaching times to obtain the flattened layers were determined for different molecular weights; their relationships with $N^{1/2}$ are shown in Figure 7b. The leaching time to obtain the flattened layer increased exponentially with increasing $N^{1/2}$. Moreover, the leaching processes and leaching times to obtain the PMMA-1 flattened layers on substrates with various OH group contents using DMF are shown in Figure S7b and Figure 7c. The leaching time decreases with decreasing OH group content on the substrate surface. A small increase in the number of contacts greatly enhanced the elution time of the loosely adsorbed chains. These results indicate that the OH groups on the substrate controlled the formation of the adsorbed layer structure. Furthermore, the physical properties (e.g., T_g) of the corresponding supported PMMA films could be tuned by adjusting the substrate surface chemistry.

CONCLUSIONS

In this paper, the structure of the PMMA adsorbed layer was adjusted by changing the OH group content on the SiO_2−Si surface. The PMMA adsorbed layer consisted of a flattened layer and loosely adsorbed chains with 100% OH group content on the SiO_2−Si substrate. With the increased displacement of OH groups by phenyl groups, both the flattened layer and loosely adsorbed layer decreased in thickness. When the OH group content on the substrate surface decreased to 31%, the flattened layer disappeared and the PMMA adsorbed layer consisted only of loosely adsorbed chains. This could be caused by the change in the content of OH groups, which served as anchoring points for the adsorption of PMMA chains because hydrogen bonds formed between the OH groups on the substrate surface and the C=O groups in PMMA. The anchoring points for PMMA adsorption decreased with decreasing OH group content on the substrate surface, which hindered the formation of the train conformation by the adsorbed PMMA chains, yielding a flattened layer. Furthermore, the greater distance between neighboring anchoring points led to loosely adsorbed chains because the phenyl groups on the substrate prevented the adsorption of the PMMA chains. This caused the flattened layer to disappear, and only loosely adsorbed chains existed in the adsorbed layer. Furthermore, the segmental dynamics of the supported PMMA films can be adjusted by changing the OH group content on the substrate and accordingly changing the structure of the adsorbed layer. This study provides a novel method to adjust the structure of the adsorbed layer; moreover, it offers insight into the formation of the adsorbed PMMA layer.

ASSOCIATED CONTENT

Supporting Information

The Supporting Information is available free of charge at https://pubs.acs.org/doi/10.1021/acs.macromol.2c02169.

Normalized thicknesses for PMMA-1 adsorbed layers as a function of temperature; thickness of the PMMA-1 interfacial sublayer as a function of annealing time; AFM height images of the PMMA-1 adsorbed layer; XRR fitting results of a four-layer model and three-layer model for the PMMA-1 interfacial sublayer; structure of the flattened layer of PMMA-1 acquired via XRR; calculated tilt angle of $-OCH_3$; residual thickness of PMMA as a function of increasing time; AFM height images and bearing area analysis results of the PMMA-2 flattened layer on various substrates; fitting parameters for the SFG spectra; Figures S1−S7; Tables S1−S3 (PDF)

https://doi.org/10.1021/acs.macromol.2c02169
Macromolecules XXXX, XXX, XXX−XXX

AUTHOR INFORMATION

Corresponding Authors

Jianquan Xu − *Department of Chemistry, Key Laboratory of Surface & Interface Science of Polymer Materials of Zhejiang Province, Zhejiang Sci-Tech University, Hangzhou 310018, China;* orcid.org/0000-0001-8554-8400; Email: jqxu@zstu.edu.cn

Xinping Wang − *Department of Chemistry, Key Laboratory of Surface & Interface Science of Polymer Materials of Zhejiang Province, Zhejiang Sci-Tech University, Hangzhou 310018, China;* orcid.org/0000-0002-9269-3275; Email: wxinping@zstu.edu.cn

Authors

Weizhao Ren − *Department of Chemistry, Key Laboratory of Surface & Interface Science of Polymer Materials of Zhejiang Province, Zhejiang Sci-Tech University, Hangzhou 310018, China*

Yongming Hong − *Department of Chemistry, Key Laboratory of Surface & Interface Science of Polymer Materials of Zhejiang Province, Zhejiang Sci-Tech University, Hangzhou 310018, China;* orcid.org/0000-0002-7735-4822

Huidong Wei − *Department of Chemistry, Key Laboratory of Surface & Interface Science of Polymer Materials of Zhejiang Province, Zhejiang Sci-Tech University, Hangzhou 310018, China*

Cuiyun Zhang − *Department of Chemistry, Key Laboratory of Surface & Interface Science of Polymer Materials of Zhejiang Province, Zhejiang Sci-Tech University, Hangzhou 310018, China*

Xianjing Zhou − *Department of Chemistry, Key Laboratory of Surface & Interface Science of Polymer Materials of Zhejiang Province, Zhejiang Sci-Tech University, Hangzhou 310018, China;* orcid.org/0000-0001-7703-7555

Complete contact information is available at: https://pubs.acs.org/10.1021/acs.macromol.2c02169

Notes

The authors declare no competing financial interest.

ACKNOWLEDGMENTS

We acknowledge the support from the National Natural Science Foundation of China (NSFC; nos. 22161160317, 22173081, and 21873085). The experimental work was supported by the Sharing Service Platform of CAS (Chinese Academy of Sciences) Large Research Infrastructures (no. 2021-SSRF-PT-015103). We also thank the staff at SSRF for their help during our experiments there.

REFERENCES

(1) Napolitano, S.; Rotella, C.; Wübbenhorst, M. Can Thickness and Interfacial Interactions Univocally Determine the Behavior of Polymers Confined at the Nanoscale? *ACS Macro Lett.* **2012**, *1*, 1189−1193.

(2) Koga, T.; Jiang, N.; Gin, P.; Endoh, M. K.; Narayanan, S.; Lurio, L. B.; Sinha, S. K. Impact of an Irreversibly Adsorbed Layer on Local Viscosity of Nanoconfined Polymer Melts. *Phys. Rev. Lett.* **2011**, *107*, No. 225901.

(3) Napolitano, S.; Wübbenhorst, M. The lifetime of the deviations from bulk behaviour in polymers confined at the nanoscale. *Nat. Commun.* **2011**, *2*, 260.

(4) Zuo, B.; Zhou, H.; Davis, M. J. B.; Wang, X.; Priestley, R. D. Effect of Local Chain Conformation in Adsorbed Nanolayers on Confined Polymer Molecular Mobility. *Phys. Rev. Lett.* **2019**, *122*, No. 217801.

(5) Sun, S.; Xu, H.; Han, J.; Zhu, Y.; Zuo, B.; Wang, X.; Zhang, W. The architecture of the adsorbed layer at the substrate interface determines the glass transition of supported ultrathin polystyrene films. *Soft Matter* **2016**, *12*, 8348−8358.

(6) Ren, W.; Wang, X.; Shi, J.; Xu, J.; Taneda, H.; Yamada, N. L.; Kawaguchi, D.; Tanaka, K.; Wang, X. The role of the molecular weight of the adsorbed layer on a substrate in the suppressed dynamics of supported thin polystyrene films. *Soft Matter* **2022**, *18*, 1997−2005.

(7) Xu, J.; Liu, Z.; Lan, Y.; Zuo, B.; Wang, X.; Yang, J.; Zhang, W.; Hu, W. Mobility Gradient of Poly(ethylene terephthalate) Chains near a Substrate Scaled by the Thickness of the Adsorbed Layer. *Macromolecules* **2017**, *50*, 6804−6812.

(8) Bai, L.; Luo, P.; Yang, X.; Xu, J.; Kawaguchi, D.; Zhang, C.; Yamada, N. L.; Tanaka, K.; Zhang, W.; Wang, X. Enhanced Glass Transition Temperature of Thin Polystyrene Films Having an Underneath Cross-Linked Layer. *ACS Macro Lett.* **2022**, *11*, 210−216.

(9) Xu, J.; Wang, X.; Chen, L.; Ao, W.; Zuo, B.; Zhang, C.; Wang, X. Spatially Heterogeneous Dynamics in Supported Ultrathin Poly-(ethylene terephthalate) Films Depend on the Thicknesses of the Film and the Adsorbed Layer. *Macromolecules* **2022**, *55*, 7110−7116.

(10) Xu, J.; Wang, X.; Bian, Z.; Wu, X.; You, J.; Wang, X. Surface crystalline structure of thin poly(l-lactide) films determined by the long-range substrate effect. *Polymer* **2022**, *256*, No. 125217.

(11) Glynos, E.; Frieberg, B.; Chremos, A.; Sakellariou, G.; Gidley, D. W.; Green, P. F. Vitrification of Thin Polymer Films: From Linear Chain to Soft Colloid-like Behavior. *Macromolecules* **2015**, *48*, 2305−2312.

(12) Jiang, N.; Shang, J.; Di, X.; Endoh, M. K.; Koga, T. Formation Mechanism of High-Density, Flattened Polymer Nano layers Adsorbed on Planar Solids. *Macromolecules* **2014**, *47*, 2682−2689.

(13) Asada, M.; Jiang, N.; Sendogdular, L.; Sokolov, J.; Endoh, M. K.; Koga, T.; Fukuto, M.; Yang, L.; Akgun, B.; Dimitrioug, M.; Satija, S. Melt crystallization/dewetting of ultrathin PEO films via carbon dioxide annealing: the effects of polymer adsorbed layers. *Soft Matter* **2014**, *10*, 6392−6403.

(14) Gin, P.; Jiang, N.; Liang, C.; Taniguchi, T.; Akgun, B.; Satija, S. K.; Endoh, M. K.; Koga, T. Revealed Architectures of Adsorbed Polymer Chains at Solid-Polymer Melt Interfaces. *Phys. Rev. Lett.* **2012**, *109*, No. 265501.

(15) Housmans, C.; Sferrazza, M.; Napolitano, S. Kinetics of Irreversible Chain Adsorption. *Macromolecules* **2014**, *47*, 3390−3393.

(16) Simavilla, D. N.; Huang, W.; Vandestrick, P.; Ryckaert, J.-P.; Sferrazza, M.; Napolitano, S. Mechanisms of Polymer Adsorption onto Solid Substrates. *ACS Macro Lett.* **2017**, *6*, 975−979.

(17) Napolitano, S. Irreversible adsorption of polymer melts and nanoconfinement effects. *Soft Matter* **2020**, *16*, 5348−5365.

(18) Barkley, D. A.; Jiang, N.; Sen, M.; Endoh, M. K.; Rudick, J. G.; Koga, T.; Zhang, Y.; Gang, O.; Yuan, G.; Satija, S. K.; Kawaguchi, D.; Tanaka, K.; Karim, A. Chain Conformation near the Buried Interface in Nanoparticle-Stabilized Polymer Thin Films. *Macromolecules* **2017**, *50*, 7657−7665.

(19) Napolitano, S.; Sferrazza, M. How irreversible adsorption affects interfacial properties of polymers. *Adv. Colloid Interface Sci.* **2017**, *247*, 172−177.

(20) O'Shaughnessy, B.; Vavylonis, D. Irreversible adsorption from dilute polymer solutions. *Eur. Phys. J. E: Soft Matter Biol. Phys.* **2003**, *11*, 213−230.

(21) O'Shaughnessy, B.; Vavylonis, D. Irreversibility and Polymer Adsorption. *Phys. Rev. Lett.* **2003**, *90*, No. 056103.

(22) Scheutjens, J. M. H. M.; Fleer, G. J. Statistical Theory of the Adsorption of Interacting Chain Molecules. 2. Train, Loop, and Tail Size Distribution. *J. Phys. Chem.* **1980**, *84*, 178−190.

(23) Zheng, F.; Zuo, B.; Zhu, Y.; Yang, J.; Wang, X. Probing substrate effects on relaxation dynamics of ultrathin poly(vinyl acetate) films by dynamic wetting of water droplets on their surfaces. *Soft Matter* **2013**, *9*, 11680−11689.

(24) Horinouchi, A.; Tanaka, K. An effect of stereoregularity on the structure of poly(methyl methacrylate) at air and water interfaces. *RSC Adv.* **2013**, *3*, 9446−9452.
(25) Tateishi, Y.; Kai, N.; Noguchi, H.; Uosaki, K.; Nagamura, T.; Tanaka, K. Local conformation of poly(methyl methacrylate) at nitrogen and water interfaces. *Polym. Chem.* **2010**, *1*, 303−311.
(26) Hong, Y.; Li, Y.; Wang, F.; Zuo, B.; Wang, X.; Zhang, L.; Kawaguchi, D.; Tanaka, K. Enhanced Thermal Stability of Polystyrene by Interfacial Noncovalent Interactions. *Macromolecules* **2018**, *51*, 5620−5627.
(27) Hong, Y.; Chen, W.; Fang, H.; Zuo, B.; Yuan, Y.; Zhang, L.; Wang, X. Regulation of the Interfacial Effects of Thin Polystyrene Films by Changing the Aromatic Group Structure on Substrate Surfaces. *J. Phys. Chem. C* **2019**, *123*, 19715−19724.
(28) Zuo, B.; Wang, F.; Hao, Z.; He, H.; Zhang, S.; Priestley, R. D.; Wang, X. Influence of the Interfacial Effect on Polymer Thin-Film Dynamics Scaled by the Distance of Chain Mobility Suppression by the Substrate. *Macromolecules* **2019**, *52*, 3753−3762.
(29) Guiselin, O. Irreversible Adsorption of a Concentrated Polymer Solution. *Europhys. Lett.* **1992**, *17*, 225−230.
(30) Hong, Y.; Zhou, H.; Qian, W.; Zuo, B.; Wang, X. Impact of the α-Methyl Group (α-CH3) on the Aggregation States and Interfacial Isotherms of Poly(acrylates) Monolayers at the Water Surface. *J. Phys. Chem. C* **2017**, *121*, 19816−19827.
(31) Hong, Y.; Bao, S.; Xiang, X.; Wang, X. Concentration-Dominated Orientation of Phenyl Groups at the Polystyrene/Graphene Interface. *ACS Macro Lett.* **2020**, *9*, 889−894.
(32) Zajac, R.; Chakrabarti, A. Irreversible polymer adsorption from semidilute and moderately dense solutions. *Phys. Rev. E: Stat. Phys., Plasmas, Fluids, Relat. Interdiscip. Top.* **1995**, *52*, 6536−6549.
(33) Buenviaje, C.; Ge, S.; Rafailovich, M.; Sokolov, J.; Drake, J. M.; Overney, R. M. Confined Flow in Polymer Films at Interfaces. *Langmuir* **1999**, *15*, 6446−6450.
(34) Durning, C. J.; O'Shaughnessy, B.; Sawhney, U.; Nguyen, D.; Majewski, J.; Smith, G. S. Adsorption of Poly(methyl methacrylate) Melts on Quartz. *Macromolecules* **1999**, *32*, 6772−6781.
(35) Jiang, N.; Cheung, J. M.; Guo, Y.; Endoh, M. K.; Koga, T.; Yuan, G.; Satija, S. K. Stability of Adsorbed Polystyrene Nanolayers on Silicon Substrates. *Macromol. Chem. Phys.* **2018**, *219*, No. 1700326.
(36) Jiang, N.; Sen, M.; Zeng, W.; Chen, Z.; Cheung, J. M.; Morimitsu, Y.; Endoh, M. K.; Koga, T.; Fukuto, M.; Yuan, G.; Satija, S. K.; Carrillo, J.-M. Y.; Sumpter, B. G. Structure-induced switching of interpolymer adhesion at a solid-polymer melt interface. *Soft Matter* **2018**, *14*, 1108−1119.
(37) Jiang, N.; Wang, J.; Di, X.; Cheung, J.; Zeng, W.; Endoh, M. K.; Koga, T.; Satija, S. K. Nanoscale adsorbed structures as a robust approach for tailoring polymer film stability. *Soft Matter* **2016**, *12*, 1801−1809.
(38) Hansen, C. M., *Hansen Solubility Parameters: A User's Handbook*. CRC Press: Boca Raton, FL, 2007.
(39) Vignaud, G.; Chebil, M. S.; Bal, J. K.; Delorme, N.; Beuvier, T.; Grohens, Y.; Gibaud, A. Densification and Depression in Glass Transition Temperature in Polystyrene Thin Films. *Langmuir* **2014**, *30*, 11599−11608.
(40) Lee, S.; Lyulin, A. V.; Frank, C. W.; Yoon, D. Y. Interface characteristics of polystyrene melts in free-standing thin films and on graphite surface from molecular dynamics simulations. *Polymer* **2017**, *116*, 540−548.
(41) Keddie, J. L.; Jones, R. A. L.; Cory, R. A. Interface and Surface Effects on the Glass-transition Temperature in Thin Polymer Films. *Faraday Discuss.* **1994**, *98*, 219−230.
(42) Roth, C. B.; McNerny, K. L.; Jager, W. F.; Torkelson, J. M. Eliminating the Enhanced Mobility at the Free Surface of Polystyrene: Fluorescence Studies of the Glass Transition Temperature in Thin Bilayer Films of Immiscible Polymers. *Macromolecules* **2007**, *40*, 2568−2574.
(43) Wang, J.; Chen, C.; Buck, S. M.; Chen, Z. Molecular Chemical Structure on Poly(methyl methacrylate) (PMMA) Surface Studied by Sum Frequency Generation (SFG) Vibrational Spectroscopy. *J. Phys. Chem. B* **2001**, *105*, 12118−12125.
(44) Clarke, M. L.; Chen, C.; Wang, J.; Chen, Z. Molecular Level Structures of Poly(n-alkyl methacrylate)s with Different Side Chain Lengths at the Polymer/Air and Polymer/Water Interfaces. *Langmuir* **2006**, *22*, 8800−8806.
(45) Jena, K. C.; Covert, P. A.; Hall, S. A.; Hore, D. K. Absolute Orientation of Ester Side Chains on the PMMA Surface. *J. Phys. Chem. C* **2011**, *115*, 15570−15574.
(46) Horinouchi, A.; Atarashi, H.; Fujii, Y.; Tanaka, K. Dynamics of Water-Induced Surface Reorganization in Poly(methyl methacrylate) Films. *Macromolecules* **2012**, *45*, 4638−4642.
(47) Xu, J.; Liu, Y.; He, J.; Zhang, R.; Zuo, B.; Wang, X. Surface structures of poly(methyl methacrylate) films influenced by chain entanglement in the corresponding film-formation solution. *Soft Matter* **2014**, *10*, 8992−9002.
(48) Gautam, K. S.; Schwab, A. D.; Dhinojwala, A.; Zhang, D.; Dougal, S. M.; Yeganeh, M. S. Molecular Structure of Polystyrene at Air/Polymer and Solid/Polymer Interfaces. *Phys. Rev. Lett.* **2000**, *85*, 3854−3857.
(49) Chen, Z. Investigating buried polymer interfaces using sum frequency generation vibrational spectroscopy. *Prog. Polym. Sci.* **2010**, *35*, 1376−1402.
(50) Tsuruta, H.; Fujii, Y.; Kai, N.; Kataoka, H.; Ishizone, T.; Doi, M.; Morita, H.; Tanaka, K. Local Conformation and Relaxation of Polystyrene at Substrate Interface. *Macromolecules* **2012**, *45*, 4643−4649.
(51) Li, B.; Zhou, J.; Xu, X.; Yu, J.; Shao, W.; Fang, Y.; Lu, X. Solvent quality affects chain conformational order at the polymer surface revealed by sum frequency generation vibrational spectroscopy. *Polymer* **2013**, *54*, 1853−1859.
(52) Li, X.; Lu, X. Evolution of Irreversibly Adsorbed Layer Promotes Dewetting of Polystyrene Film on Sapphire. *Macromolecules* **2018**, *51*, 6653−6660.
(53) Inutsuka, M.; Horinouchi, A.; Tanaka, K. Aggregation States of Polymers at Hydrophobic and Hydrophilic Solid Interfaces. *ACS Macro Lett.* **2015**, *4*, 1174−1178.
(54) Jenckel, E.; Rumbach, B. Über die Adsorption von hochmolekularen Stoffen aus der Lösung. *Z. Elektrochem. Angew. Phys. Chem.* **1951**, *55*, 612−618.
(55) Sen, M.; Jiang, N.; Cheung, J.; Endoh, M. K.; Koge, T.; Kawaguchi, D.; Tanaka, K. Flattening Process of Polymer Chains Irreversibly Adsorbed on a Solid. *ACS Macro Lett.* **2016**, *5*, 504−508.
(56) Reiter, G.; Schultz, J.; Auroy, P.; Auvray, L. Improving adhesion via connector polymers to stabilize non-wetting liquid films. *Europhys. Lett.* **1996**, *33*, 29−34.
(57) Reiter, G.; Auroy, P.; Auvray, L. Instabilities of Thin Polymer Films on Layers of Chemically Identical Grafted Molecules. *Macromolecules* **1996**, *29*, 2150−2157.
(58) Raphael, E.; De Gennes, P. G. Rubber-Rubber Adhesion with Connector Molecules. *J. Phys. Chem.* **1992**, *96*, 4002−4007.
(59) Aubouy, M.; Fredrickson, G. H.; Pincus, P.; Raphaeel, E. End-Tethered Chains in Polymeric Matrixes. *Macromolecules* **1995**, *28*, 2979−2981.
(60) Zuo, B.; Zhang, S.; Niu, C.; Zhou, H.; Sun, S.; Wang, X. Grafting density dominant glass transition of dry polystyrene brushes. *Soft Matter* **2017**, *13*, 2426−2436.

https://doi.org/10.1021/acs.macromol.2c02169
Macromolecules XXXX, XXX, XXX−XXX